Wideband Pattern-Reconfigurable Antenna with Switchable Broadside and Conical Beams

Wei Lin, *Member, IEEE*, Hang Wong, *Senior Member, IEEE* and Richard W. Ziolkowski, *Fellow, IEEE*

***Abstract*— A wideband, pattern-reconfigurable antenna is reported that is, for example, a good candidate for ceiling mounted indoor wireless systems. Switchable linearly polarized broadside and conical radiation patterns are achieved by systematically integrating a wideband low-profile monopolar patch antenna with a wideband L-probe fed patch antenna. The monopolar patch acts as the ground for the L-probe fed patch, which is fed with a coaxial cable that replaces one shorting via of the monopolar patch to avoid deterioration of the conical-beam pattern. A simple switching feed network facilitates the pattern reconfigurability. A prototype was fabricated and tested. The measured results confirm the predicted wideband radiation performance. The operational impedance bandwidth, i.e., $|S_{11}| \leq -10$ dB, is obtained as the overlap of the bands associated with both pattern modalities. It is wide, from 2.25 to 2.85 GHz (23.5%). Switchable broadside and conical radiation patterns are observed across this entire operating bandwidth. The peak measured gain was 8.2 dBi for the broadside mode and 6.9 dBi for the conical mode. The overall profile of this antenna is $0.13\lambda_0$ at its lowest operating frequency.**

***Index Terms*— broadside pattern, conical pattern, patch antennas, pattern-reconfigurable antennas, reconfigurable antennas, wideband**

I. Introduction

Pattern-reconfigurable antennas have drawn much attention with the rapid development of modern wireless communication systems. They have many advantageous features including increased radiation coverage, enhanced wireless channel capacity, and enabled beam-sweeping for point-to-multipoint communications [1] – [5]. Pattern-reconfigurable antennas can be classified generally into two categories: continuously sweeping beams and discrete switching between pattern shapes. Antennas with continuous beam sweeping characteristics usually adopt tunable components, such as varactors, to continuously adjust the main beam direction [6], [7]. These systems are useful for object tracking, e.g., for radar applications. On the other hand, reconfigurable antennas that switch their radiation patterns in a discrete manner utilize RF switches.

An antenna that is switchable between distinct conical-beam and broadside-beam patterns enables enhanced radiation coverage. In addition, this diversity feature also facilitates an increase of the system capacity as has been demonstrated in a MIMO setting [8]. One typical application is an indoor wireless network for coverage within a large crowded train station hall, e.g. Central Station in Sydney, as shown in Fig. 1. To realize the largest radiation coverage, ceiling mounted antennas are desired that have both omni-directional conical-beam and uni-directional broadside-beam patterns. The latter beam fills in the hole of the pattern of the former. This approach avoids undesirable fade zones in which the wireless signal is very weak.

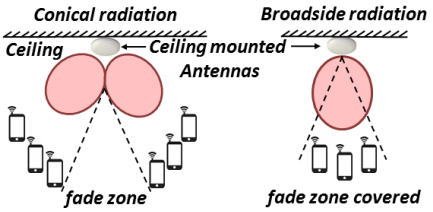

Fig. 1. Ceiling-mounted wireless indoor communication systems facilitated by the reported pattern-reconfigurable antenna with switchable broadside and conical radiation patterns.

Several pattern-reconfigurable antenna designs have been reported, e.g., [9] – [13], that emphasize broadside and conical beams. However, their overall performance characteristics are not satisfactory. For instance, the square-ring patch antenna in [9] gives switchable broadside and conical patterns, but it only has a 2.5% impedance (-10dB) bandwidth. The designs in [10] and [11] are able to switch between patch and monopole modes; they have slightly larger bandwidths: 6.6% and 7.6%, respectively. But the cost is a gain discrepancy larger than 3 dB between the two modes. Another design [12] realized similar pattern reconfigurability, by switching between monopole and dipole modes in the presence of a reflector, and similar bandwidth, 6.5%, but produced unacceptable measured radiation patterns. To increase the bandwidth to 9%, the antenna design in [13] employed convertible slot and monopolar patch modes. Nonetheless, the monopolar mode pattern was bi-directional, which gave poor omni-directional radiation coverage.

In this letter, we present a wideband (23.5%), pattern-reconfigurable antenna by systematically integrating a monopolar patch and an L-probe fed patch together. Novel excitation techniques are designed to generate the broadside and conical patterns. The realized operating bandwidth is more than twice as large as other reported designs, and the realized gain values are higher and more stable in both pattern modes.

II. Antenna Design

To realize a wideband broadside and conical pattern reconfigurability, a wideband monopolar patch is systematically integrated with a wideband L-probe fed patch. The resulting antenna system is excited with a switchable feeding network.

A. Antenna Configuration

The antenna consists of three parts as shown in Fig. 1. It includes an L-probe fed circular patch antenna (top layer), a center-fed monopolar patch antenna (middle layer), and a switching feeding network (bottom layer). The circular L-probe fed patch is placed concentrically with the monopolar patch with a separation distance H_{patch}. It is air-loaded and has the diameter D_{patch}. The length and the height of the L-probe are, L_{probe} and H_{probe}, respectively. Their values and the location of the L-probe, R_{probe}, are optimized to achieve a wide bandwidth impedance match. The center-fed monopolar patch has the diameter D_m. It serves as the ground for the L-probe fed patch when the system is in its broadside radiation mode and as the main radiator when it is in its conical radiation mode. The monopolar patch is also air loaded and concentrically located above the ground at the distance H_m. There are seventeen vias uniformly distributed along a circle whose radius is R_{pin}. Each via has the diameter D_{pin}. Sixteen are selected to be shorted between the monopolar patch and the ground. The seventeenth is replaced with a small piece of coaxial cable feedline which is used to excite the L-shaped probe. It does not go directly through the cavity of the monopolar patch; it is connected to a small piece of microstrip transmission line etched on a rectangular piece of metal-clad dielectric substrate (labeled as *Substrate_L-probe)*. The switching feeding network is etched on the bottom surface of another concentrically located, circular metallic-clad dielectric substrate disk labeled as *Substrate_feeding*. It has the diameter D_{ground}. The top surface of this disk is the metallic ground for the monopolar patch. Both of the metal-clad dielectric substrates are manufactured by *Wangling Ltd*; each has a relative permittivity of 2.65, loss tangent of 0.001 and 1.0 mm thickness. Finally, two 3D-printed fixtures and several plastic screws are used to provide the mechanical stability of the entire antenna structure. The key, optimized design parameter values are (in millimeters):
H_{patch} = 10, D_{patch} = 52, L_{probe} = 24.5, H_{probe} = 4.5, R_{probe} = 30.5, D_m = 124, D_{pin} = 1, R_{pin} = 45.8, H_m = 6, and D_{ground} = 170.

B. Switching Mechanism

To realize the pattern reconfigurability, PIN diodes are introduced as the RF switches in a simple feeding network which selects the excitation paths between the monopolar patch and the L-probe fed patch. The arrangement of the PIN diodes is presented in Fig. 2. The PIN diodes selected were model number Bar50-02L with 0403 surface mount packaging from Infineon Technologies. They have excellent switching performance below 6 GHz. The measured characteristics and equivalent circuit models were reported previously [14] – [16]. The total DC power consumption of this PIN diode is 12 mW, i.e., $P_{dc} = I^2 R = (100\ mA)^2 \times 1.2\ \Omega$ as calculated from its datasheet [17]. In addition, the Murata inductors: Type LQW 18AN56NJ00 with 0603 packaging, were selected as the RF chokes.

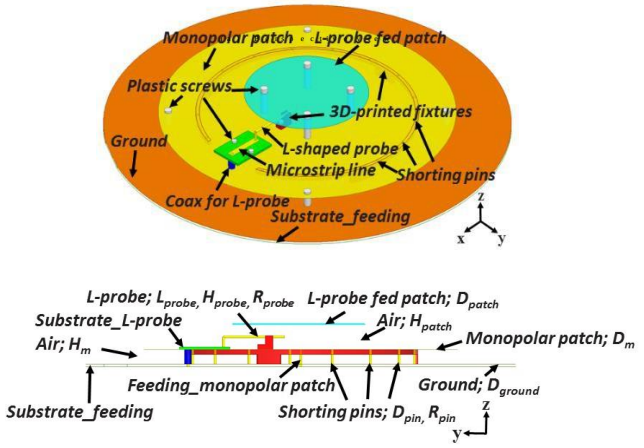

(b) Side view without supporting plastic posts

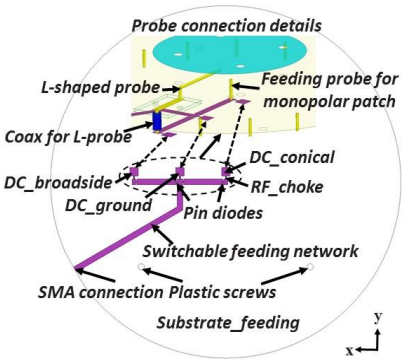

(c) Bottom view

Fig. 1. Pattern-reconfigurable antenna: (a) perspective view, (b) side view without the supporting plastic posts, and (c) bottom view.

To control the diode states, three DC bias voltages are needed. They are labeled as *DC_broadside*, *DC_conical* and *DC_ground*. The detailed connections of these DC biases are shown in both Fig. 1(c) and Fig. 2. The radiation modes are simply changed by applying different DC voltages as shown in Table I. For example, if the two green diodes are turned-on by applying the DC voltages: 3V to *DC_broadside* and 0V to *DC_ground*, but leaving the other two red diodes turned-off, the broadside radiation mode is generated. Similarly, the conical radiation mode is obtained by switching the positive DC voltage to *DC_conical*. From the current distributions given in Fig. 3, one can clearly see that the L-probe fed patch is excited in the broadside mode while the monopolar patch is excited in the conical mode. Thus the desired pattern reconfigurability is achieved by switching between these two states. The wideband characteristics are realized because the L-shaped probe is able to compensate for the large inductance of the probe-fed patch [17]. Furthermore, the shorting vias help merge the TM_{01} and TM_{02} modes together in the monopolar patch radiator [14].

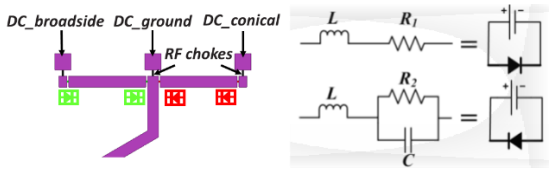

Fig. 2. (Left) Arrangement of the diodes in the simple feeding network and their DC bias pads and labels. (Right) Equivalent circuit of the PIN diode.

TABLE I: DC bias values that yield the broadside and conical beams

DC_broadside	*DC_conical*	*DC_ground*	Pattern mode
3 V	N/A	0 V	Broadside
N/A	3 V	0 V	Conical

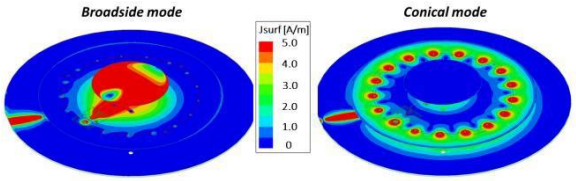

Fig. 3. Current distributions on the antenna elements when the system is operating in its broadside (left) and conical (right) modes.

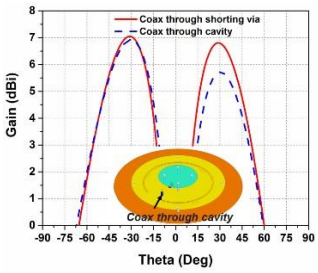

Fig. 4. Comparison of the radiation patterns in the vertical plane $\varphi = 0°$ plane when the coax center conductor replaces one of the seventeen shorting vias versus when it goes directly going through the cavity of the monopolar patch.

C. *Impact of coax feed position*

Despite the straightforward nature of the design, the small piece of coaxial cable is indispensable. It connects the microstrip feedline on the bottom layer to the L-probe on the middle layer. Again, as depicted in Fig. 1, the coax does not go through the monopolar patch cavity directly below the L-probe. Rather, it replaces the 17th shorting pin. This specific design is adopted to avoid the deterioration of either the TM_{01} or TM_{02} mode within the cavity of the monopolar patch. An asymmetry would exist if the coax were to go directly through the cavity, producing non-uniform electric fields along the perimeter of the monopolar patch and, hence, an asymmetrical conical radiation pattern. As Fig. 4 shows, the discrepancy between the two sides of the conical beam is larger than 1 dB when the coax goes directly through the cavity. On the other hand, it shows that there is little difference when the outer conductor of the coax goes through the position of one shorting pin.

III. Measured Results

The optimized pattern-reconfigurable antenna were fabricated. The assembled prototype is shown in Fig. 5. The reflection coefficients were measured with a Keysight Vector Network Analyzer. The radiation patterns were measured in a SATIMO Starlab near-field measurement system.

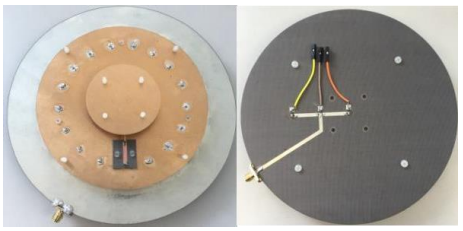

Fig. 5. Photos of the fabricated prototype.

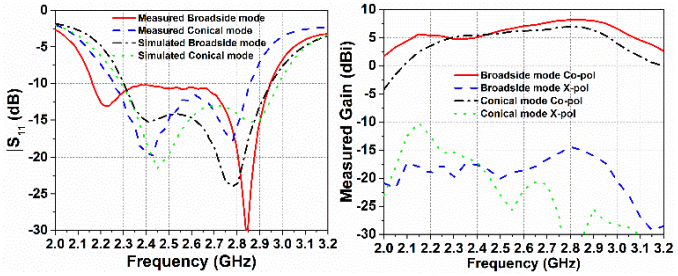

Fig. 6. (Left) Measured and simulated $|S_{11}|$ values for both the broadside and the conical radiation modes. (Right) Measured realized gain values for the broadside and conical radiation modes.

A comparison of the measured and simulated $|S_{11}|$ values is given in Fig. 6. The measured overlap of the bandwidths associated with both modes is wide, 23.5%, from 2.25 to 2.85 GHz. The mild discrepancies between the measured and simulated results occur in part from small fabrication inaccuracies and from the actual impedances of the PIN diodes. In particular, the impedance matching of the two modes is very sensitive to the dimensions and the positions of the L-probe and the shorting pins as discussed in [18] and [19]. Moreover, since all the components are manually assembled, the agreement level is quite reasonable. The difference in the wider measured bandwidth is only 150 MHz (5.8%) for the broadside mode and 100 MHz (3.9%) for the conical mode.

The measured peak realized gain values for both radiation modes as functions of the source frequency are presented in Fig. 7. The gain variation is stable (less than 3 dB) across the entire operating bandwidth. The peak gain for the broadside mode is 8.2 dBi and for the conical mode is 6.9 dBi. The gain discrepancy between the broadside and conical modes is less than 1.3 dB and the cross polarization level ratio is larger than 20 dB across the entire operating bandwidth. The measured average total radiation efficiency is 66% and 75% for the broadside and conical mode, respectively.

The measured radiation patterns are given in Fig. 8. They confirm that switchable, wideband broadside and conical radiation patterns were realized. The patterns are symmetrical for both vertical ($\phi = 0°$ and 90°) planes and are stable across the entire operating bandwidth.

Table II provides a summary of the measured performance characteristics of comparable pattern-reconfigurable antennas. Our larger design achieves the largest operating bandwidth and

the highest peak realized gain. Additionally, the differences between the realized gain and total efficiency values of both modes is small and very low cross-pol levels are maintained. Furthermore, the fabrication complexity of our design is modest in comparison. Given all of these advantages, the size tradeoff is reasonable.

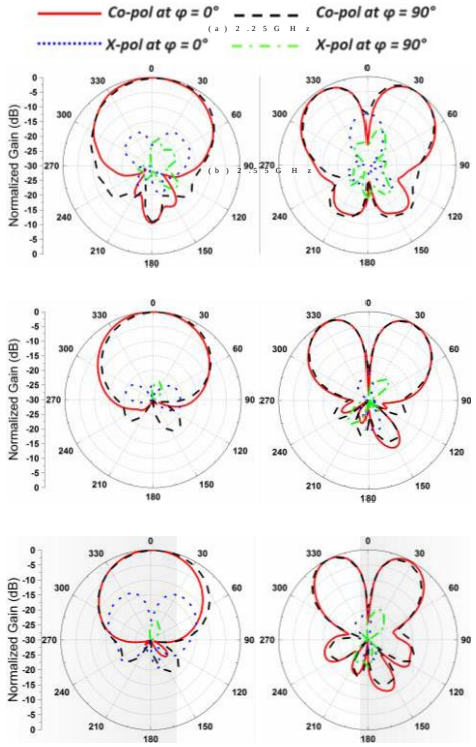

Fig. 8. Measured radiation patterns in the two orthogonal vertical planes for both the broadside and conical radiation modes at the center frequency, 2.55 GHz, and at the two edge frequencies: 2.25 and 2.85 GHz.

IV. Conclusion

A wideband, pattern-reconfigurable antenna was reported. It has switchable broadside and conical radiation patterns. The design strategy was discussed in detail. A prototype was fabricated and tested. The measured results confirmed its wide bandwidth and switchable radiation patterns. This pattern-reconfigurable antenna is a very good candidate, e.g., as a ceiling mounted antenna for indoor wireless applications.

Acknowledgments

The authors would like to thank Prof. Y. Jay Guo from the University of Technology Sydney (UTS) for his support pertaining to the work reported in this letter. The authors would also like to thank Mr. C. K Lau from the City University of Hong Kong for the fabrication of the metallic parts of the antenna. This work was supported in part by the Australian Research Council grant number DP160102219 and in part by the Research Grants Council of the Hong Kong SAR, China (Project No. CityU 11216915).

TABLE II
Comparson of Pattern-Reconfigurable (Brside, Conical) Antennas

Ref.	BW (%)	Gain (dBi)	Total Eff. (%)	Cross Pol. Level (dBi)	Total Size (λ_0^3)
[9]	2.5	6.8, 2.5	75, 60	-20, -20	0.67×0.67×0.05
[10]	6.6	6.5, 4.0	87, 45	-40, -20	0.88×0.88×0.06
[12]	6.5	5.3, 2.6	68, 76	NA	0.65×0.69×0.06
[13]	9	4.1, 4.8	NA	NA	0.51×0.39×0.01
This work	**23.5**	**8.2, 6.9**	**66, 75**	**-25, -30**	**1.28×1.28×0.13**

V. References

[1] J. T. Bernhard, Reconfigurable Antennas, London, UK: Morgan & Claypool, 2007.

[2] M. C. Tang, B. Y. Zhou and R. W. Ziolkowski, "Low-profile, electrically small, huygens source antenna With pattern-reconfigurability that covers the entire azimuthal plane," *IEEE Trans. Antennas Propag.*, vol. 65, no. 3, pp. 1063-1072, Mar. 2017.

[3] C. G. Christodoulou, Y. Tawk, S. A. Lane and S. R. Erwin, "Reconfigurable antennas for wireless and space applications," *Proc. IEEE*, vol. 100, pp. 2250-2261, July 2012.

[4] N. Nguyen-Trong, L. Hall, and C. Fumeaux, "A frequency- and pattern-reconfigurable center-shorted microstrip antenna," *IEEE Antennas Wireless Propag. Lett.*, vol. 15, pp. 1955-1958, 2016.

[5] L. Ge, K. M. Luk and S. C. Chen, "360° Beam-Steering Reconfigurable Wideband Substrate Integrated Waveguide Horn Antenna," *IEEE Trans. Antennas Propag.*, vol. 64, no. 12, pp. 5005-5011, Oct. 2016.

[6] S. V. Hum, M. Okoniewski and R. J. Davies, "Modeling and design of electronically tunable reflectarrays," *IEEE Trans. Antennas Propag.*, vol. 55, no. 8, pp. 2200-2210, Aug. 2007.

[7] T. Debogović and J. P. Carrier, "Array-fed partially reflective surface antenna with independent scanning and beamwidth dynamic control," *IEEE Trans. Antennas Propag.*, vol. 62, no. 1, pp. 446-449, Jan. 2014.

[8] J. D. Boerman and J. T. Bernhard, "Performance study of pattern reconfigurable antennas in MIMO communication systems," *IEEE Trans. Antennas Propag.*, vol. 56, no. 1, pp. 231–236, Jan. 2007.

[9] S. H. Chen, J. S. Row and K. L. Wong, "Reconfigurable square-ring patch antenna with pattern diversity," *IEEE Trans. Antennas Propag.*, vol. 55, no. 2, pp. 472-475, Feb. 2007.

[10] P. Y. Qin, Y. J. Guo, A. R. Weily and C. H. Liang, "A pattern reconfigurable U-slot antenna and its applications in MIMO systems," *IEEE Trans. Antennas Propag.*, vol. 60, no. 2, pp. 516-528, Feb. 2012.

[11] H. Zhong, Z. Zhang, W. Chen, Z, Feng and M. F. Iskander, "A tripolarization antenna fed by proximity coupling and probe," *IEEE Antennas Wireless Propag. Lett.*, vol. 8, pp. 465-467, 2009.

[12] W. S. Kang, J. A. Park and Y. J. Yoon, "Simple reconfigurable antenna with radiation pattern," *Electro. Lett.*, vol. 44, no. 3, Jan. 2008.

[13] I. Lim and S. Lim, "Monopole-like and boresight pattern reconfigurable antenna," *IEEE Trans. Antennas Propag.*, vol. 61, no. 12, pp. 5854-5859, Dec. 2013.

[14] W. Lin and H. Wong, "Polarization reconfigurable wheel-shaped antenna with conical-beam radiation pattern," *IEEE Trans. Antennas Propag.*, vol. 63, no. 2, pp. 491–499, Feb. 2015.

[15] W. Lin and H. Wong, "Polarization reconfigurable aperture-fed patch antenna and array," *IEEE Access*, vol. 4, pp. 1510-1517, Apr. 2016.

[16] L. Ge, X. Yang, D. Zhang, M. Li, and H. Wong, "Polarization-Reconfigurable Magnetoelectric Dipole Antenna for 5G Wi-Fi", *IEEE Antennas and Wireless Propagation Letters*, vol. 16, pp. 1504-1507, 2017.

[17] Data Sheet of Bar50-02L PIN Diodes, Infineon Technologies, Application Note [Online]. Available: http://www.infineon.com/.

[18] H. Wong, K. L. Lau and K. M. Luk, "Design of dual-polarized L-probe patch antenna arrays with high isolation," *IEEE Trans. Antennas Propag.*, vol. 52, no. 1, pp. 45–52, Jan. 2004.

[19] W. Lin and H. Wong, "Circularly polarized conical beam antenna with very thin profile and wide bandwidth," *IEEE Trans. Antennas Propag.*, vol. 62, no. 12, pp. 5974-5982, Dec. 2014.